# A lattice spring model of heterogeneous materials with plasticity

BUXTON, G. A., CARE, C. M. and CLEAVER, D. J. <http://orcid.org/0000-0002-4278-0098>



**Published version**

BUXTON, G. A., CARE, C. M. and CLEAVER, D. J. (2001). A lattice spring model of heterogeneous materials with plasticity. Modelling and simulation in materials science and engineering, 9 (6), 485-497.

# A lattice spring model of heterogeneous materials with plasticity

Gavin A. Buxton, Christopher M. Care and Douglas J. Cleaver

Materials Research Institute, Sheffield Hallam University, Pond Street, Sheffield S1 1WB, United Kingdom.

**Abstract**

A three dimensional lattice spring model of a heterogeneous material is presented. For small deformations, the model is shown to recover the governing equations for an isotropic elastic medium. The model gives reasonable agreement with theoretical predictions for the elastic fields generated by a spherical inclusion, although for small particle sizes the discretisation of the underlying lattice causes some departures from the predicted values. Plasticity is introduced by decreasing the elastic moduli locally whilst maintaining stress continuity. Results are presented for a spherical inclusion in a plastic matrix and are found to be in good agreement with predictions of Wilner [1].

# 1 Introduction

An understanding of the deformation and fracture processes within engineering materials is of practical interest in the design of reliable structural components. The initial process by which a material fails is often dictated by the statistical nature of the microstructural components responsible for crack nucleation, such as grain boundaries and second phase particulates [2]. In order to elucidate the essential physics of material failure, the influence of such constituents must be investigated. The elastic response of an ellipsoidal inhomogeneity, in an otherwise elastic homogeneous media, was solved analytically by Eshelby [3, 4, 5]. However, in order to describe plasticity and progressive damage, numerical solutions are required. Finite-element methods (FEM) and lattice spring models (LSM) have emerged as numerical methods for analysing the continuum mechanics of a material's microstructure. LSM have been shown to be algebraically equivalent to simple finite-element methods [6] in which the lattice springs are analogous to element boundaries and linear interpolations functions are utilised [7].

The majority of FEM microstructural investigations employ pre-processed mesh generation, allowing the mesh to be refined at key areas of interest, i.e. particle interface or crack tip. This has enabled FEM simulations of particulate systems to be obtained [8, 9, 10, 11, 12, 13]; generally unit cell models are considered, were the distribution of particles is assumed to be periodic. FEMs include the possibility of introducing non-linear material deformations, although crack initiation is usually predetermined and involves expensive, and subjective, remeshing procedures.

LSM are adopted from condensed matter physics as a method of discretising continuum elastic media and are frequently used to simulate deformation and fracture. In the simulation of elastic-brittle systems, the spatial co-operative effects of crack formation and heterogeneities are easily investigated through the use of LSM [14]. A LSM consists of a regular two- or three-dimensional network of one-dimensional springs. A variety of LSM have been developed, distinguishable via the hamiltonian associated with nodal interactions. The simplest formulation can be considered as an electrical equivalent to elasticity (force is comparable to current, displacement to voltage, and stiffness to conductance); static equilibrium is determined through the solution of a system of equations equivalent to Kirchoff's law [15, 16, 17, 18, 19, 20]. Hookean spring models, consisting of a network of springs which exhibit central force interactions, allow a constant Poisson's ratio to be obtained [21, 22]. The Poisson's ratio can be modified by introducing a harmonic potential for rotation of bonds from

their initial orientation [23]; the Born spring model introduces a non-central two-body interaction limiting the rotational freedom of bonds [24, 25, 26]. However rotational invariance of the models can only be recovered if an orientational potential is introduced through a three-body potential. The Kirkwood-Keating spring model includes a central force interaction and an additional term which energetically penalises the angular variation between two neighbouring bonds [27, 28, 29, 7]. It is unclear if the nonlinearity introduced through the angular terms, when linearised for subsequent solution, offer any advantage over the Born spring model. The implementation may be more equivalent to the iterative rotation of the localised equilibrium orientation in a Born model, in which case the additional computational expense is unwarranted. In the systems considered, rotations are assumed to be small, and therefore a Born spring model is implemented in the present study.

The simulation of heterogeneous materials is achieved through assigning force constants to individual bonds depending upon the phase in which they appear [30] and thereby avoiding complicated mesh generation. The majority of particulate simulations have been two-dimensional investigations of circular [31, 32, 33, 14, 34] and fibre [35, 29] inclusions, although a spherical particle has been investigated in a three-dimensional simulation [36]. The regularity of LSM networks can result in stress anomalies along the particle surface [33] which can be partially alleviated through the introduction of interfacial bonds whose characteristics are apportioned according to the weighting of the partial lengths of the bond that straddles the respective domains [30, 34]. LSM can be used to investigate the physics of stress transfer and stress field redistribution in complicated heterogeneous systems which arise from inhomogeneities and damage accumulation; the latter being simulated through element removal. The system is iteratively relaxed to the minimum energy configuration, transferring forces from broken bonds to nearest neighbour bonds. Various criteria for element removal have been investigated, including critical elastic stress, strain, or energy [21, 23, 29], and less deterministic approaches [37, 38, 39]. LSM are predominantly associated with the simulation of brittle fracture, although attempts to include plasticity have been undertaken [40, 41, 42, 43]. Plasticity is commonly associated with the springs and this results in intrinsically anisotropic plastic deformation which does not recover conservation of volume.

In this paper we present a direct comparison of the results of an LSM simulation of a particulate with the analytical predictions of Eshelby [3, 4, 5]. The LSM is then extended to include isotropic plasticity and the results

are compared with other numerical methods in the literature. In all cases it is shown that the LSM is in good agreement with the alternative methods and therefore provides a computationally efficient technique for modelling heterogeneous materials.

# 2 The Model.

The elastic and plastic response of the material is represented by an array of 'springs' which occupy the nearest, and next nearest neighbour, bonds of a simple cubic lattice (see Figure 1). The energy associated with a node $m$ in the lattice is assumed to be of the form,

$$E_m = \frac{1}{2}\sum_n (\mathbf{u}_m - \mathbf{u}_n).\mathbf{M}_{mn}.(\mathbf{u}_m - \mathbf{u}_n) \tag{1}$$

where the summation is over all the neighbouring nodes, $n$, attached to $m$ by a spring, $\mathbf{u}_m$ is the displacement of node $m$, and $\mathbf{M}_{mn}$ is a symmetric matrix which determines the elastic properties of the springs. It is shown in the subsequent parts of this section that this system of springs obeys, to first order, the equations of continuum elastic theory for an isotropic elastic medium whose elastic constants can be determined in terms of the elements of the matrices $\mathbf{M}_{mn}$.

The harmonic form of the energy (1) results in forces which are linearly dependent upon the displacement of the nodes and the resulting set of sparse linear equations may be solved by a conjugate gradient method to find the equilibrium configuration which corresponds to no net force at each node. The matrices $\mathbf{M}_{mn}$ associated with a bond can be varied to represent the material properties present in different phases within the same material, hence allowing heterogeneous systems to be simulated. Bonds which straddle two phases are assigned linearly interpolated values. The response of the system can be determined by iteratively increasing the applied forces at the boundary nodes and fracture can be introduced though the iterative removal of bonds.

## 2.1 Form of the spring matrices

We assume that the matrix associated with the spring in the [100] direction is of the form

$$\mathbf{M}_{[100]} = \begin{pmatrix} k_1 & 0 & 0 \\ 0 & c_1 & 0 \\ 0 & 0 & c_1 \end{pmatrix} \tag{2}$$

In this matrix, $k_1$ and $c_1$ correspond respectively to extensional and rotational force constants. We construct the matrices corresponding to the springs in the equivalent symmetry directions by a similarity transformation of the form

$$\mathbf{M}' = \mathbf{R}.\mathbf{M}.\mathbf{R}^T \tag{3}$$

where $\mathbf{R}$ is the rotation matrix which rotates a vector in the [100] direction into the required direction. In addition the matrices corresponding to the set of directions $\{110\}$ have the force constants $(c_1, k_1)$ replaced by $(k_2, c_2)$. Hence, for example, the matrix corresponding to the [110] direction is

$$\mathbf{M}_{[110]} = \begin{pmatrix} \frac{1}{2}(k_2 + c_2) & \frac{1}{2}(k_2 - c_2) & 0 \\ \frac{1}{2}(k_2 - c_2) & \frac{1}{2}(k_2 + c_2) & 0 \\ 0 & 0 & c_2 \end{pmatrix} \tag{4}$$

In the following analysis we consider a homogeneous material in which only the force constants $(k_1, k_2, c_1, c_2)$ are used. It is now shown how these constants may be chosen in order to recover an isotropic elastic medium.

## 2.2 Free energy

In order to correctly represent the elastic properties of a medium which is described by the spring model described above we must generalise the free energy normally associated with an elastic medium [44] to include contributions from an anti-symmetric strain tensor because the model is not rotationally invariant. This arises because the bond bending terms give rise to an energy which depends upon the absolute orientation of the bonds. The problem may be avoided [35] by expressing the energy in a form which depends only upon the angles between the bonds rather than the absolute orientation, as is used in equation (1). However this latter approach yields a significantly more complex set of equations to solve and becomes computationally prohibitive when considering fracture in heterogeneous materials in the presence of plasticity.

The most general quadratic form of the free energy of an elastic continuum which is not rotationally invariant may be written in the form

$$A = \frac{1}{2}\lambda_{iklm}\epsilon_{ik}\epsilon_{lm} + \frac{1}{2}\gamma_{iklm}\omega_{ik}\omega_{lm} + \frac{1}{2}\eta_{iklm}\omega_{ik}\epsilon_{lm} \tag{5}$$

where $\epsilon_{ik}$ is the symmetric strain tensor and $\omega_{ik}$ is the anti-symmetric strain tensor and the three tensors $\lambda, \gamma$ and $\eta$ are material parameters. For a three

dimensional system with simple cubic symmetry, it is possible to show that this equation reduces to

$$\begin{aligned} A &= b_1(\epsilon_{xx}^2+\epsilon_{yy}^2+\epsilon_{zz}^2)+b_2(\epsilon_{xx}\epsilon_{yy}+\epsilon_{yy}\epsilon_{zz}+\epsilon_{zz}\epsilon_{xx}) \\ &\quad +b_3(\epsilon_{xy}^2+\epsilon_{yz}^2+\epsilon_{zx}^2)+d_1(\omega_{xy}^2+\omega_{yz}^2+\omega_{zx}^2) \end{aligned} \tag{6}$$

where the constants $\{b_1, b_2, b_3, d_1\}$ determine the elastic properties of the material and the term pre-multiplied by $d_1$ introduces anti-symmetric contributions to the stress tensor. Extending standard arguments, [44], it can be shown that

$$dA = -SdT + \sigma_{ik}^S d\epsilon_{ik} + \sigma_{ik}^A d\omega_{ik} \tag{7}$$

where

$$\sigma_{ik} = \sigma_{ik}^S + \sigma_{ik}^A \tag{8}$$

with the symmetric and anti-symmetric contributions to the stress tensor being given from equation (7) by

$$\sigma_{ik}^S = \left(\tfrac{\partial A}{\partial \epsilon_{ik}}\right)_T \qquad \sigma_{ik}^A = \left(\tfrac{\partial A}{\partial \omega_{ik}}\right)_T \tag{9}$$

At equilibrium, in the absence of body forces, we must have

$$F_i = \frac{\partial \sigma_{ik}}{\partial x_k} = 0 \tag{10}$$

which give the following Lamé equations

$$\begin{aligned} 2b_1\partial_x^2 u_x + (b_2+\frac{b_3}{2}-\frac{d_1}{2})(\partial_x\partial_y u_y+\partial_x\partial_z u_z)+(\frac{b_3}{2}+\frac{d_1}{2})(\partial_y^2 u_x+\partial_z^2 u_x) &= 0 \\ 2b_1\partial_y^2 u_y + (b_2+\frac{b_3}{2}-\frac{d_1}{2})(\partial_y\partial_x u_x+\partial_y\partial_z u_z)+(\frac{b_3}{2}+\frac{d_1}{2})(\partial_x^2 u_y+\partial_z^2 u_y) &= 0 \\ 2b_1\partial_z^2 u_z + (b_2+\frac{b_3}{2}-\frac{d_1}{2})(\partial_z\partial_x u_x+\partial_z\partial_y u_y)+(\frac{b_3}{2}+\frac{d_1}{2})(\partial_x^2 u_z+\partial_y^2 u_z) &= 0 \end{aligned} \tag{11}$$

For a medium with a free energy given by equation (6) undergoing an extension in the direction $\hat{\mathbf{n}} = (n_x, n_y, n_z)$, it can be shown that the Young's modulus is given by

$$\begin{aligned} E &= \left[\frac{2b_1+b_2}{2(2b_1-b_2)(b_1+b_2)}\right. \\ &\quad \left.+(n_x^2n_y^2+n_y^2n_z^2+n_z^2n_x^2)\left(\frac{2(2b_1-b_2-b_3)}{b_3(2b_1-b_2)}\right)\right]^{-1} \end{aligned} \tag{12}$$

and the Poisson's ratio by

$$\nu = \frac{\left[\left(-\frac{b_2 b_3}{(b1+b_2)} + 4(2b_1 - b_2 - b_3)(n_x m_x n_y m_y + n_y m_y n_z m_z + n_z m_z n_x m_x)\right)\right]}{\left[\frac{(2b_1+b_2)b_3}{(b_1+b_2)} + 4(2b_1 - b_2 - b_3)(n_x^2 n_y^2 + n_y^2 n_z^2 + n_z^2 n_x^2\right]} \tag{13}$$

Hence if the constants $b_i$ are such that $b_1 = (b_2 + b_3)/2$, the system becomes isotropic and

$$E = \frac{b_3(3b_2+b_3)}{2b_2+b_3} \qquad \nu = -\frac{b_2}{2b_2+b_3} \tag{14}$$

If we make the identifications $b_1 = \frac{1}{2}(\lambda + 2\mu)$, $b_2 = \lambda$ and $b_3 = 2\mu$ where $\lambda$ and $\mu$ are the Lamé coefficients, we recover the standard results for the Young's modulus $E$ and Poisson's ratio $\nu$ for a three dimensional isotropic material

$$E = \frac{\mu(3\lambda + 2\mu)}{(\lambda + \mu)} \qquad \nu = -\frac{\lambda}{2(\lambda + \mu)} \tag{15}$$

### 2.3 Mapping of the spring model onto continuum equations

In order to map the spring model onto the continuum equations we make the Taylor approximation

$$\begin{aligned} \mathbf{u}_m - \mathbf{u}_n &\approx \mathbf{u}(x + (c_{mn})_x, y + (c_{mn})_y) - \mathbf{u}(x, y) \\ &\approx (\mathbf{c}_{mn}.\nabla)\mathbf{u}(x, y) + \frac{1}{2}(\mathbf{c}_{mn}.\nabla)^2\mathbf{u}(x, y) \end{aligned} \tag{16}$$

where $\mathbf{u}(x, y)$ is the vector displacement field of a two dimensional continuum material and $\mathbf{c}_{mn}$ are the bond vectors (*not* unit vectors). We may use this expansion in the expression $\mathbf{F}_m = \sum_n \mathbf{M}.(\mathbf{u_n} - \mathbf{u_n})$ for the force on node $m$ and derive the form of the Lamé equations for the spring model. Alternatively an expression for the energy density can be derived using the Taylor approximation (16) in the energy $E_m$ given by equation (1). If we equate coefficients in these equations with those in for the elastic continuum (equations (6) and (11)), and assume the primitive cell of the simple cubic lattice has unit side, we find the following relationships between the elastic constants of the continuum and spring models

$$\begin{aligned} b_1 &= \tfrac{1}{2}(k_1 + 2k_2 + 2c_2) & b_2 &= k_2 - c_2 \\ b_3 &= 2k_2 + c_1 + 2c_2 & d_1 &= c_1 + 4c_2 \end{aligned} \tag{17}$$

It is important to note that although the term $d_1$ associated with the antisymmetric contribution to the free energy does not affect the elastic constants, it is essential for the term to be included if the mapping onto the continuum equations using the free energy expression and the Lamé equations are to be consistent. In order for the spring model to become isotropic we require $2b_1 = b_2 + b_3$ and for simplicity we choose and $k_2 = k_1$ and $c_2 = c_1$ and hence the spring model has the following properties

$$\mathbf{M}_{[100]} = \begin{pmatrix} k & 0 \\ 0 & c \end{pmatrix} \qquad \mathbf{M}_{[110]} = \frac{1}{2}\begin{pmatrix} k+c & k-c \\ k-c & k+c \end{pmatrix} \tag{18}$$

$$\lambda = (k - c) \qquad \mu = \frac{1}{2}(2k + 3c) \tag{19}$$

and hence

$$E = \frac{5k(2k+3c)}{4k+c} \qquad \nu = \frac{k-c}{c+4k} \qquad K = \frac{3\lambda + 2\mu}{3} = \frac{5k}{3} \tag{20}$$

where $K$ is the bulk modulus and we note that the Poissons' ratio has an upper bound of $\frac{1}{4}$.

## 2.4 Introduction of plasticity

In order to expand the range of materials that can be simulated using the LSM, the present formulation is extended to include continuum plasticity. In reality, the shape of the yield surface has a complex load history dependence [45], and this results in anisotropic hardening characteristics. For simplicity we consider a system with which undergoes isotropic hardening, in which the yield surface expands isotropically (proportional loading) [46]; this is valid, assuming reasonably small variations in the principal directions of applied stress.

In the present study the Ramberg-Osgood stress-strain relation is adopted from Wilner [1], which incorporates a plastic strain field, $\varepsilon_{ij}^p$, of the form

$$\varepsilon_{ij}^p = \frac{9}{14}\left(\frac{\sigma_{eq}}{\sigma_1}\right)^{n-1}\frac{\sigma_{ij}^{'}}{E} \tag{21}$$

where $\sigma_1$ is the plastic resistance, and $n$ is the hardening exponent. The plastic response of the material depends upon the equivalent stress, $\sigma_{eq}$, and the deviatoric stress tensor, $\sigma_{ij}^{'} = \sigma_{ij} - \frac{1}{3}\delta_{ij}\sigma_{ll}$, both of which are undefined for a single bond. Attempting to introduce plasticity through bond dependent criteria results in anisotropic plasticity and, therefore, in this

work the plastic response is controlled by the stress fields calculated at each node.

In order to maintain the linearity of the model defined in section (2), the plastic response of the material is modelled by decreasing the elastic moduli locally whilst maintaining stress continuity. Thus the force constants of the springs are modified at each iteration, with the modifications being determined by the elastic fields from the previous iteration. The continuity of stress is achieved by incorporating internal forces applied at each node. The force constant for each spring is calculated from the elastic fields at its terminal nodes as shown below.

After each iteration the stress field, $\sigma_{ij}$, is calculated at each node and hence the equivalent stress, $\sigma_{eq}$. These quantities are used to determine the required value of the strain tensor in the presence of plastic deformation from the relation

$$\varepsilon_{ij} = \frac{\delta_{ij}\sigma_{ll}}{9K} + \frac{\sigma'_{ij}}{2\mu} + \frac{9}{14}\left(\frac{\sigma_{eq}}{\sigma_1}\right)^{n-1}\frac{\sigma'_{ij}}{E} \tag{22}$$

where the constants $K$ and $\mu$ are elastic constants which determine the elastic response of the target material. In order to mimic the combined elastic and plastic response, we set the force constants of the bond to be $k^T$ and $c^T$ which are chosen to be equivalent to a material which obeys the relation

$$\frac{\partial \varepsilon_{ij}}{\partial \sigma_{lm}} = \frac{\partial}{\partial \sigma_{lm}}\left(\frac{\delta_{ij}\sigma_{ll}}{9K^T} + \frac{\sigma'_{ij}}{2\mu^T}\right) \tag{23}$$

This recovers the required differential response of the stress-strain curve. In order to maintain continuity of stress as the bond parameters are modified, an additional force is applied to each end of the spring whose value $\psi_{mn}$ is given by

$$\psi_{mn} = \mathbf{F}'_{mn} - \mathbf{M}^T_{mn}(\mathbf{u}_m - \mathbf{u}_n) \tag{24}$$

where $\mathbf{M}^T_{mn}$ is the bond matrix with the force constants $k^T$ and $c^T$ and $\mathbf{F}'_{mn}$ is the force which is currently applied to the bond.

With increasing plastic deformation, the Poisson's ratio is found experimentally to increase to a value close to half and hence corresponds to a volume conserving deformation. However the current model is restricted to a Poisson's ratio with an upper bound of a quarter and hence the observed deformation in this scheme is isotropic, but not volume conserving. In order to rectify this problem a volume conservation term will be required [47]. However, the dominant aspect of plastic deformation is assumed to be the reduction in Young's modulus and therefore the present procedure is considered adequate for the situations considered here.

# 3 Results and discussion.

## 3.1 Simulation of an elastic inhomogeneity problem.

In this section, an elastically heterogeneous material is simulated using the LSM described above . The deformation of an elastic matrix containing an elastic particle is simulated and a direct comparison of the resultant elastic fields is made with those predicted by Eshelby's analytical solution [5, 4, 3] to the inhomogeneity problem. The particle considered is spherical and is introduced through the assignment of different force constants depending upon whether a bond appears in the region associated with the matrix or within the particle; particle-matrix interfacial bonds are assigned elastic properties according to the weighting of the bonds partial lengths straddling the respective domains.

The ratio of particle to matrix Young's modulus is chosen to be four; this is large enough to represent many real particulate systems. The Poisson's ratio is considered to be of secondary importance and therefore a quarter is assigned to both phases. A system with $81 \times 81 \times 81$ nodes is considered and the boundaries in the $x$ direction are subject to forces equivalent to an applied uniaxial stress field. The force is chosen to give a far field strain corresponding to four percent in the absence of an inclusion. The disturbance of the elastic fields due to the particle are influenced by the uniformity of the boundary stress, a problem which becomes significant if the particle is placed too close to the boundary. It should also be noted that the linearity of the LSM implies that the magnitude of the elastic fields, relative to far field values, are independent of the magnitude of the applied stress.

Two-dimensional profiles through the centre of the particle are presented (Figures 2 and 3), displaying the normal component of the stress and strain tensors ($\sigma_{11}$ and $\varepsilon_{11}$). Both fields show concentrations at the particle interface along the pole, in the tensile direction, and relaxation along the interface in the equatorial plane, perpendicular to the tensile direction. Discretisation effects are present at the interface, resulting in field anomalies, whilst the far field response appears regular. The fields are predicted by Eshelby to be uniform within the particle and the data is essentially consistent with this result; within the particle the normal stress field is concentrated above the applied stress whilst the normal strain field is relaxed.

In order to assess the model quantitatively, the field variations along the polar axis of the particle in the tensile direction are considered (Figure 4). This direction is chosen since the fields exhibit the largest

changes in this direction. In addition to the normal stress ($\sigma_{11}$) and normal strain ($\varepsilon_{11}$), results are presented for the free energy, $F_E = \frac{1}{2}\sigma_{ij}\varepsilon_{ij}$, the Mises stress, $\sigma_{eq} = \left(\frac{3}{2}\sigma'_{ij}\sigma'_{ij}\right)$ and the hydrostatic stress, $\sigma_H = \frac{1}{2}(\sigma_{ii})$. In all cases the fields, $F$, are scaled with respect to the uniform far fields, $F_0$; $r$ is the position along the pole and $a$ is the particle radius.

The simulation results are compared with the theoretical predictions of Eshelby [3, 4, 5] and are seen to be in reasonable agreement. It is believed that the discrete nature of the representation of the spherical particle leads to the main disagreement with the theoretical predictions. The normal strain and the free energy have been calculated in a central difference approximation, and have difficulty in capturing the discontinuity exhibited in both fields. It is possible that this effect could be reduced through the appropriate use of forward or backward approximations at the particle interface. By comparison, the stress field is calculated at each node and is able to follow the predicted discontinuity more accurately.

The simulation adequately replicates the elastic fields both within the particle and the far field response, and is therefore considered suitable for simulating multiple particulate systems. In reality the particles are not perfectly spherical, and consequently the elastic field anomalies arising from the discretisation of the elastic material in the vicinity of a particle are considered to be acceptable for use in the simulation of particulate systems.

### 3.2 Elastic inclusion in plastic matrix

In this section we present results for an elastic inclusion embedded within a plastic matrix. Of particular importance in real materials is the inability of elastic inclusions to deform to the same extent as a plastically deforming matrix. This can be the source of internal necking in particulate systems leading to premature failure. In order to incorporate the micromechanical behaviour of such systems into LSM, plasticity must first be introduced. The incipient stages of plastic deformation around an elastic inclusion are simulated. The system considered is directly comparable to that studied by Wilner in which equation (21) reduces, for uniaxial stress strain behaviour, to the relation [1]

$$\epsilon = \frac{\sigma}{E}\left[1 + \frac{3}{7}\left(\frac{\sigma}{\sigma_1}\right)^{n-1}\right]. \tag{25}$$

The ductility is dependent upon the hardening exponent, $n$, and the plastic resistance, $\sigma_1$, which are assigned values of 19 and 1, respectively, characteristic of a considerably ductile response. The initial elastic properties are also

taken from Wilner and consist of particle to matrix Young's moduli ratio of two and a Poison's ratio of a quarter for both phases. The plastic zone is defined as being a region were the Mises stress is greater than the plastic resistance; in order to interpret the slight deviations in the results from those of Wilner, only the range of Mises stress between $0.99\sigma_1$ and $1.01\sigma_1$ is considered in Figure 5. From symmetry it is only necessary present data for one quadrant of the contour map.

The onset of plastic deformation is related to a critical Mises stress and therefore the initial plastic zone is expected to develop where the maximum Mises stress occurs (Figure 4); this is generally observed in the literature at a position separate from the particle [48, 49, 8]. In the present simulation this phenomenon is not fully captured, due to the discretisation of the particle, and the plastic zone develops at the interface of the particle (Figure 5a). Increasing the applied stress (Figures 5b to 5d) results in further growth of the plastic zone along the line of loading, and hence a local increase in deformation, causing an increase in Mises stress at roughly $r/a \approx 2$ in the equatorial plane. Comparable phenomenon have been observed using FEM [9, 50], although in direct comparison with the numerical results of Wilner [1](based on a variational method), the effect within the LSM simulation do not appear as pronounced; this is attributed to the lack of volume conservation in the plastic zone along the pole in the tensile direction. Another discrepancy with the results of Wilner is the effect of the boundary conditions in the LSM upon the Mises stress profile. In the LSM the applied far field imposes a constant normal stress contour along the boundary, which curbs the Mises stress profile. That said, the model captures the essential features of the evolution of the plastic zone and are clearly very similar to those reported by Wilner [1].

# 4 Summary and Conclusions.

The formulation of a LSM of both elasticity and plasticity has been presented. The elastic formulation is achieved through the direct comparison of the elastic free energy of the LSM with that of an isotropic continuum. The plasticity is introduced through the localised modification of elastic constants, maintaining stress field continuity. Numerical simulation of the elastic inhomogeneity problem, utilising a LSM, has been undertaken and it is found that the analytical solutions of Eshelby are accurately replicated, although the discretisation of a spherical particle results in elastic field anomalies at the particle-matrix interface. In order to extend the range of

materials that can be simulated with LSM, a method for inclusion of the plastic deformation into the formulation have been developed. It is found that the onset of plastic deformation agrees well with that determined using alternative methods.

The LSM presented in this paper is capable of simulating the elastic-plastic deformation of heterogeneous systems and extension of LSM to include damage is straightforward. The principal advantage of the LSM method presented in this work is computational simplicity. In future work, the effects of particle clustering in heterogeneous sytems will be studied through the direct simulation of multi-particle systems. Subsequent analysis of the spatial co-operative effects associated with randomly located heterogeniety and damage accumulation will offer significant insights into the micromechanical origins of macromechanical behaviour.

## References


[1] B.Wilner. *J. Mech. Phys. Solids*, 36:2:141–165, 1988.

[2] J.F.Knott. *Fundamentals of Fracture Mechanics*. The Butterworth Group, 1973.

[3] J.D.Eshelby. *Proc. Roy. Soc. A*, 241:376–396, 1957.

[4] J.D.Eshelby. *Proc. Roy. Soc. A*, 252:561–569, 1959.

[5] J.D.Eshelby. *Prog. Solid Mech.*, 2:88–139, 1961.

[6] W.T.Ashurst and W.G.Hoover. *Phys. Rev. B*, 14:4:1465–1473, 1976.

[7] P.Y.Sheng M.Ostoja-Starzewski and K.Alzebdeh. *Comp. Mater. Sci*, 7:82–93, 1996.

[8] R.D.Thompson and J.W.Hancock. *Int. J. Fracture*, 24:209–228, 1984.

[9] C.L.Hom and R.M.McMeeking. *Int. J. Plasticity*, 7:255–274, 1991.

[10] C.L.Hom. *J. Mech. Phys. Solids*, 40:5:991–1008, 1992.

[11] X.Q.Xu and D.F.Watt. *Acta Metall. Mater.*, 42:11:3717–3729, 1994.

[12] X.Q.Xu and D.F.Watt. *Acta Mater.*, 44:2:801–811, 1996.

[13] X.Q.Xu D.F.Watt and D.J.Lloyd. *Acta Mater.*, 44:2:789–799, 1996.

[14] P.Y.Sheng M.Ostoja-Starzewski and I.Jasuik. *Engng. Fract. Mech.*, 58:5-6:581–606, 1997.

[15] M.C.Stephens and M.Sahimi. *Phys. Rev. B*, 36:16:8656–8659, 1987.

[16] S.Redner L.de Arcangelis B.Khang, G.G.Batrouni and H.J.Herrmann. *Phys. Rev. B*, 37:13:7625–7637, 1988.

[17] L.de Arcangelis and H.J.Herrmann. *Phys. Rev. B*, 39:4:2678–2684, 1989.

[18] J.Schmittbuhl and S.Roux. *Modelling Simul. Mater. Sci. Engng.*, 2:21–52, 1994.

[19] G.Pijaudier-Cabot A.Delaplace and S.Roux. *J. Mech. Phys. Solids*, 44:1:99–136, 1996.

[20] A.Vespignani S.Zapperi and H.E.Stanley. *Nature*, 388:14:658–660, 1997.

[21] P.D.Beale and D.J.Srolovitz. *Phys. Rev. B*, 37:10:5500–5507, 1988.

[22] D.J.Srolovitz. *J. Am. Ceram. Soc.*, 71:5:362–369, 1988.

[23] G.N.hassold and D.J.Srolovitz. *Phys. Rev. B*, 39:13:9273–9281, 1989.

[24] G.Li H.Yan and L.M.Sander. *Europhys. Lett.*, 10:1:7–13, 1989.

[25] C.Castellano G.Caldarelli and A.Petri. *Physica A*, 270:15–20, 1999.

[26] G.Caldarelli A.Parisi and L.Pietronero. *Physica A*, 280:161, 2000.

[27] M.F.Thorpe L.M.Schwartz, S.Feng and P.N.Sen. *Phys. Rev. B*, 32:7:4607–4617, 1985.

[28] M.Sahimi and S.Arbabi. *Phys. Rev. Lett.*, 68:5:608–611, 1992.

[29] L.Monette and M.P.Anderson. *Modelling Simul. Mater. Sci. Eng*, 2:53–66, 1994.

[30] P.Y.Sheng M.Ostoja-Starzewski and I.Jasuik. *J. Engng. Mater. Tech.*, 116:384–391, 1994.

[31] E.J.Garoczi K.A.Snyder and A.R.Day. *J. Appl. Phys.*, 72:12:5948–5955, 1992.

[32] L.Monette and M.P.Anderson. *Scripta Metall. et Mater.*, 28:9:1095–1100, 1993.

[33] M.P.Anderson L.Monett and G.S.Grest. *J. Appl. Phys*, 75:2:1155–1170, 1994.

[34] I.Jasuik K.Alzebdeh, A.Al-Ostaz and M.Ostoja-Starzewski. *Int. J. Solids Structures*, 35:19:2537–2566, 1998.

[35] S.Ling L.Monette, M.P.Anderson and G.S.Grest. *J. Mater. Sci*, 27:4393–4405, 1992.

[36] A.Sauron. *Computer Modelling of Crack Growth in Rubber-Toughened Polymers*. Ph.D. Thesis, Sheffield hallam university, 1997.

[37] Y.Termonia and D.J. Walsh. *J. Mater. Sci.*, 24:247–251, 1989.

[38] P.Meakin. *Science*, 252:226–233, 1991.

[39] M.Vujosevic and D.Krajcinovic. *Int. J. Solids Structures*, 34:9:1105–1122, 1997.

[40] F.Guinea M.P.Lopez-Sancho and E.Louis. *J. Phys. A*, 21:L1079–L1083, 1988.

[41] S.Roux and A.Hansen. *J. Phys. II France*, 2:1007–1021, 1992.

[42] M.E.J.Kattunen M.J.Alava and K.J.Niskanen. *Europhys. Lett.*, 32:2:143–148, 1995.

[43] V.I.Raisanen E.T.Seppala and M.J.Alava. *Phys. Rev. E*, 61:6:6312–6319, 2000.

[44] L.D.Landau and E.M.Lifshitz. *Theory of Elasticity*. Peragmon Press, 1970.

[45] J.Lemaitre and J-L.Chaboche. *Mechanics of Solid Materials*. Cambridge U.P., 1990.

[46] P.F.Thomason. *Ductile Fracture of Metals*. Pergamon Press, 1990.

[47] R.A.Johnson. *Phys. Rev. B*, 6:6:2094–2100, 1972.

[48] W.C.Johnson. *J. Appl. Mech*, 49:312–318, 1982.

[49] A.Roatta. *Mater. Sci. Engng.*, A229:182–191, 1997.

[50] A.Needleman J.Llorca and S.Suresh. *Acta Metall. Mater.*, 39:10:2317–2335, 1991.

**Figure 1.** Interconnectivity of the lattice spring model is depicted; nearest {100} and next-nearest {110} neighbour spring interactions are considered.

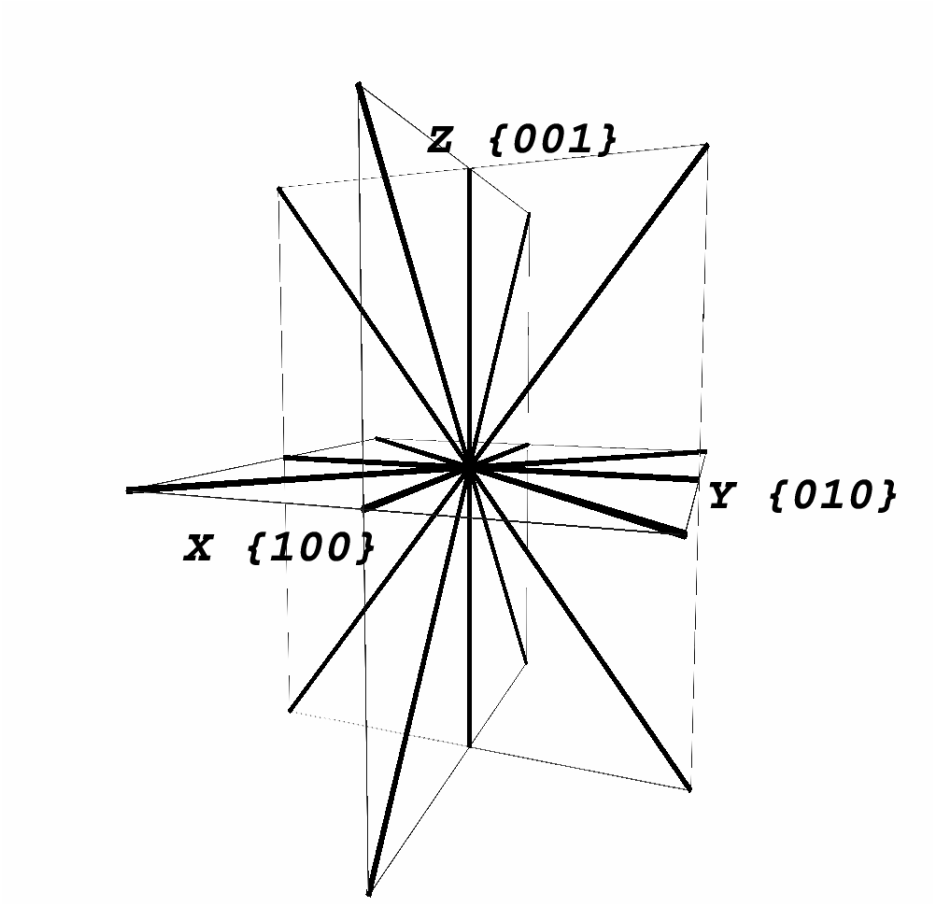

**Figure 2.** Linear elastic: normal stress profile through centre of particle (diameter is 21 unit lengths) in a system of size $L^3 = 80^3$. The horizontally applied stress corresponds to a far field uniaxial strain of four percent. The ratio of particle to matrix Young's modulus is four and the Poisson's ratio for both phases is a quarter.

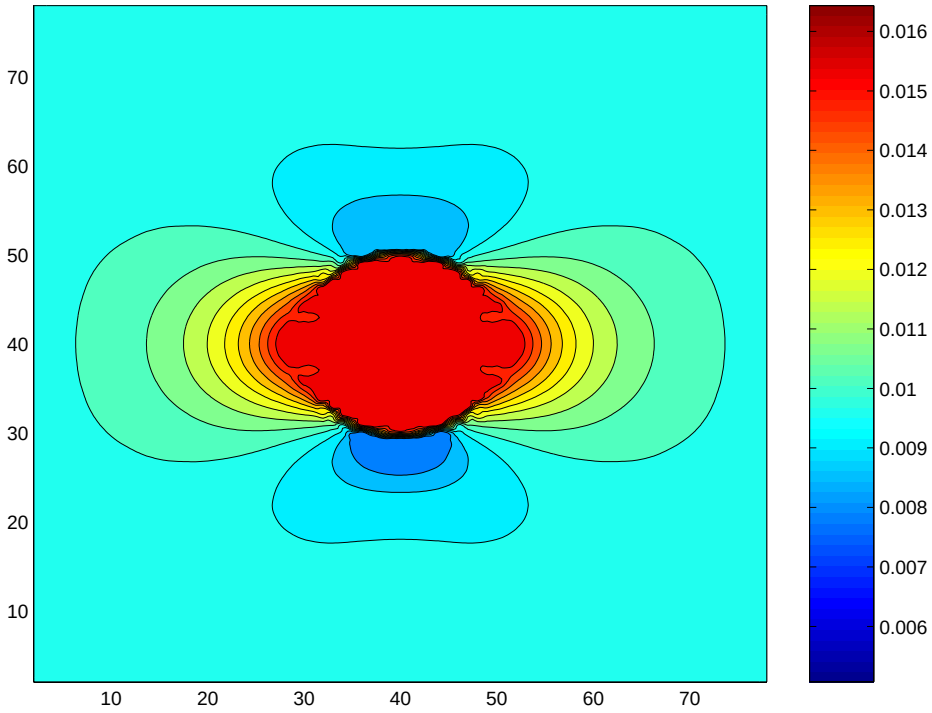

**Figure 3.** Linear elastic: normal strain profile through centre of particle (diameter is 21 unit lengths) in a system of size $L^3 = 80^3$. The horizontally applied stress corresponds to a far field uniaxial strain of four percent. The ratio of particle to matrix Young's modulus is four and the Poisson's ratio for both phases is a quarter.

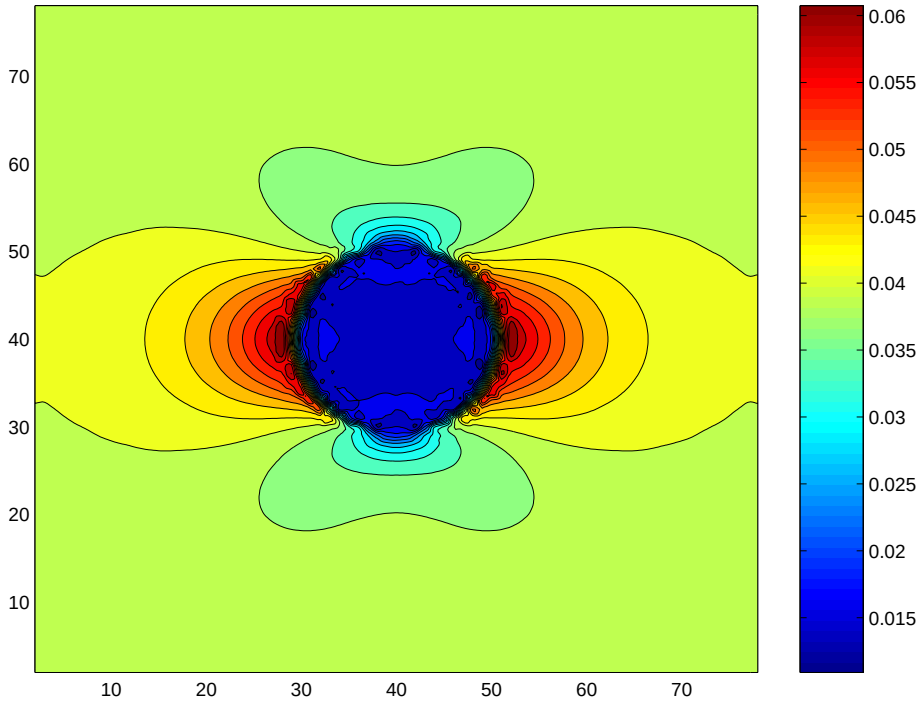

**Figure 4.** Linear elastic: various elastic parameters along the line of loading through the particle pole (diameter is 13 unit lengths) in a system of size $L^3 = 80^3$. The ratio of particle to matrix Young's modulus is four and the Poisson's ratio for both phases is a quarter. The simulation results are plotted as points, whilst the theory is plotted as lines.

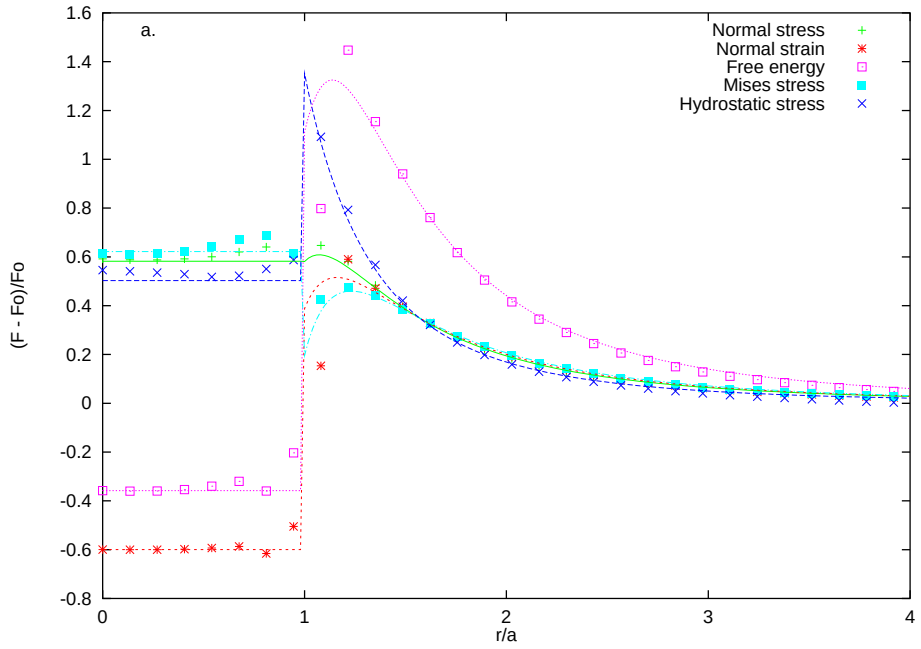

**Figure 5.** Non-linear plastic: Mises stress profile exhibiting the onset and growth of plastic zone (defined as $\sigma_{eq} = 1$). The ratio of particle to matrix Young's modulus is two, both phases are assigned a Poisson's ratio of a quarter, and the hardening exponent is nineteen. The particle diameter is thirteen unit lengths, and the vertically applied stress is a) $\sigma/\sigma_1 = 0.95$, b) $\sigma/\sigma_1 = 0.9975$, c) $\sigma/\sigma_1 = 1.0$, and d) $\sigma/\sigma_1 = 1.005$.

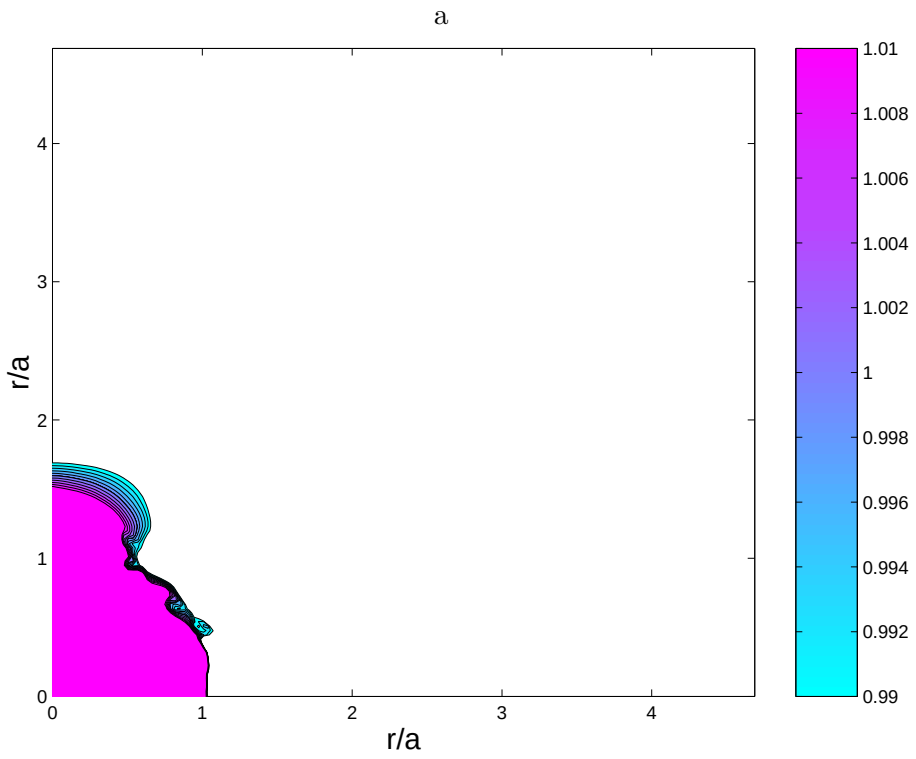

b

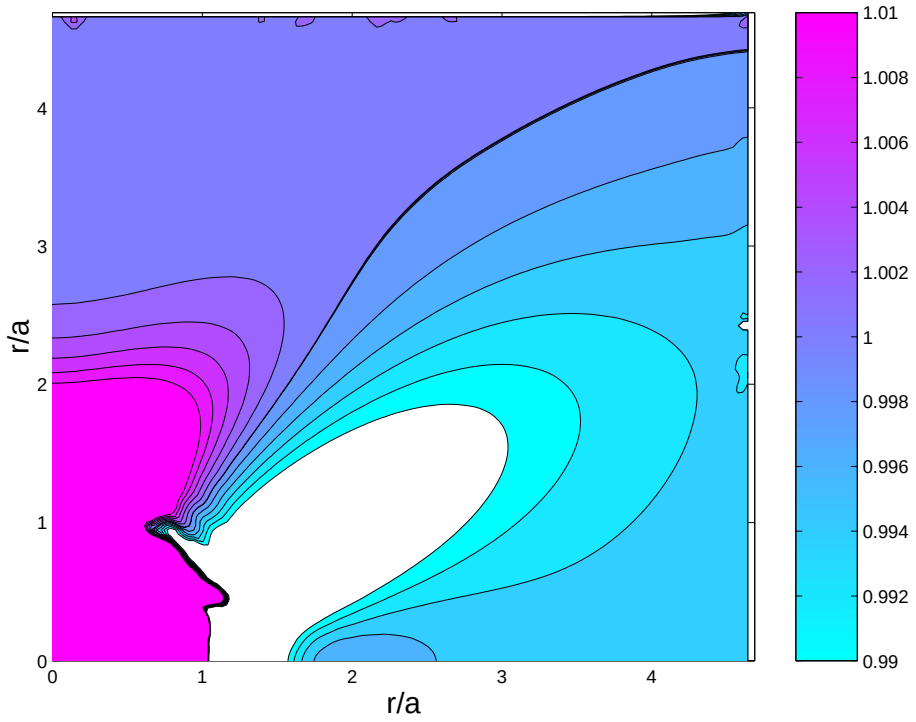

c

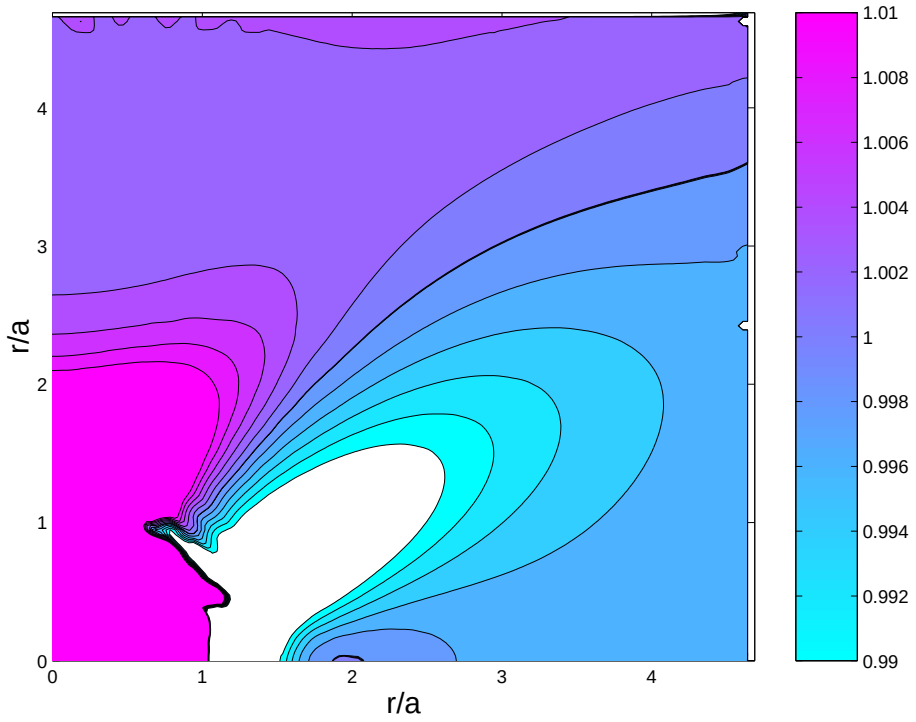

d